Interaction of low-energy electrons with dimethyl sulfide and dimethyl disulfide

J. S. dos Santos,[1] F. Kossoski,[2] and M. T. do N. Varella[2]
[1]*Universidade Federal do ABC, Centro de Ciências Naturais e Humanas, CEP 09210-170 Santo André, São Paulo, Brazil*
[2]*Instituto de Física, Universidade de São Paulo, Caixa Postal 66318, 05314-970 São Paulo, São Paulo, Brazil*
(Received 18 September 2014; published 14 November 2014)

We report elastic integral cross sections for low-energy electron scattering by gas-phase dimethyl sulfide and dimethyl disulfide, obtained with the Schwinger multichannel method with pseudopotentials. Our symmetry-resolved cross sections for dimethyl sulfide reveal that the single broad structure at 3.25 eV observed in the electron transmission spectrum (assigned as a σ^*_{CS} shape resonance) would actually arise from two superimposed anion states in the B_2 and A_1 symmetry components of the C_{2v} point group. We also obtained two low-lying shape resonances for dimethyl disulfide, in good agreement with the available electron transmission data. In view of the recently reported measurements on dissociative electron attachment to dimethyl disulfide [C. Matias, A. Mauracher, P. Scheier, P. Limão-Vieira, and S. Denifl, Chem. Phys. Lett. **605-606**, 71 (2014)], we also calculated cross sections for stretched S–S bond lengths, which indicate a fast stabilization consistent with the experimental data.

DOI: 10.1103/PhysRevA.90.052713 PACS number(s): 34.80.Bm, 34.80.Gs

I. INTRODUCTION

Sulfur containing species play a major role in a variety of metabolic processes and, more generally, in the chemistry of life. In particular, S–S bridges between cysteine residues take part in protein folding and stabilization of the secondary structure, as the formation of S–S bonds favors the folding and reduces the conformational entropy [1,2]. In addition, the role of sulfur molecules in atmospheric chemistry has been addressed in several studies [3–7].

As far as the interaction with electrons is concerned, the highly polarizable sulfur atoms would be expected to give rise to long-lived and dissociative σ^*_{SS} transient anion states. In fact, the disulfide bond cleavage in proteins and peptides can be induced either by electron transfer from negatively charged radicals [8] or by free electrons, as in electron capture dissociation mass spectroscopy [9]. In the gas phase, sulfur containing molecules give rise to σ^*_{SC} and σ^*_{SS} shape resonances with sizable dissociative electron attachment (DEA) cross sections in the latter case [10,11].

Dimethyl sulfide (DMS) and dimethyl disulfide (DMDS) (shown in Fig. 1) are important prototype systems for biophysics and biochemistry, being the subject of many computational and experimental studies. In particular, the reported electron transmission (ET) spectra of DMS [12,13] indicate a shape resonance at 3.25 eV, which was assigned to electron attachment to the lowest unoccupied molecular orbital (LUMO), having σ^*_{SC} character. In DMDS the ET spectrum [13] supports a lower-lying shape resonance at 1.04 eV, with a prevailing σ^*_{SS} character, and a higher-lying σ^*_{SC} shape resonance at 2.72 eV. Rydberg electron transfer and negative ion photoelectron spectroscopy studies indicate that the geometrically relaxed ground states of the anionic saturated disulfides *R*S–S*R* (*R* = methyl, ethyl, propyl) are slightly stable (0.1 eV), i.e., the adiabatic electron affinities are slightly positive [14]. Calculations performed with different electronic structure techniques by Gámez *et al.* [15,16] indicated that the extra electron occupies a σ^*_{SS} orbital in the DMDS anion. The DEA spectrum of DMDS was reported by Modelli *et al.* [10] and more recently by Matias *et al.* [11]. Below 1 eV, both measurements detected high yields for the SCH_2^- and SCH_3^- fragments, the most abundant being SCH_2^-, and much smaller signals for $S_2CH_3^-$, strongly indicating the electron-induced cleavage of the disulfide bond. At higher energies, the latter report [11] also pointed out additional fragments not detected in the previous account [10].

Despite the importance of disulfide bonds in several biochemical processes and the role that electrons might play in these processes, to our knowledge the theoretical results reported to date are concerned with the adiabatic anion energies, as obtained from bound-state calculations. In this sense, the collisional processes and the resonance spectra of disulfides have been somewhat disregarded on the theory side. In the present paper we report computed integral cross sections (ICS's) for elastic collisions of electrons with DMS and DMDS, for impact energies up to 12 eV. The calculations were performed with the Schwinger multichannel method (SMC) implemented with pseudopotentials. We considered the equilibrium geometries of both molecules, as well as stretched S–S bond lengths for DMDS. This paper is organized as follows. The SMC method and the computational procedures are outlined in Sec. II. Our results are presented and discussed in Sec. III, and the conclusions are summarized in Sec. IV.

II. THEORY AND COMPUTATION

The scattering calculations were performed with the parallel version [17] of the Schwinger multichannel method [18–20] implemented with pseudopotentials [21]. The SMC variational approach and its implementation are discussed in detail elsewhere [19–21], so we only outline the aspects that are relevant to the present calculations. The working expression for the scattering amplitude is given by

$$f(\mathbf{k}_i,\mathbf{k}_f) = -\frac{1}{2\pi}\sum_{m,n}\left\langle S_{\mathbf{k}_f}\middle|V\middle|\chi_m\right\rangle (d^{-1})_{mn}\left\langle\chi_n\middle|V\middle|S_{\mathbf{k}_i}\right\rangle, \quad (1)$$

where

$$d_{mn} = \langle\chi_m|A^{(+)}|\chi_n\rangle, \quad (2)$$

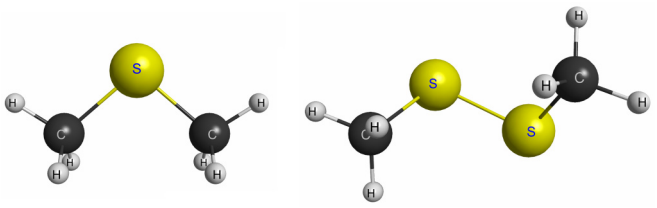

FIG. 1. (Color online) Dimethyl sulfide (DMS) on the left and dimethyl disulfide (DMDS) on the right.

and

$$A^{(+)} = \left(\frac{\hat{H}}{N+1} - \frac{\hat{H}P + P\hat{H}}{2} + \frac{PV + VP}{2} - VG_P^{(+)}V \right). \tag{3}$$

In the expressions above, P is a projector onto energy-allowed target electronic channels, $G_P^{(+)}$ is the free-particle Green's function projected onto P space, V is the projectile-target interaction potential, and $\hat{H} = (E - H)$ is the collision energy minus the scattering Hamiltonian given by $H = H_0 + V$, where H_0 describes the noninteracting electron-molecule system. $S_{\mathbf{k}}$ is a solution of H_0, and χ_m's are $(N+1)$-particle configuration state functions (CSF's), given by spin-adapted products of target electronic states and projectile scattering orbitals, which provide the basis set for expansion of the trial scattering wave function.

The present study is limited to elastic collisions, such that the open-channel projector is given by $P = |\Phi_0\rangle\langle\Phi_0|$, where Φ_0 is the target ground state. In the static-exchange (SE) approximation, the N-electron target is not allowed to respond to the field of the projectile, and CSF's are given by

$$|\chi_p\rangle = \mathcal{A}|\Phi_0\rangle|\varphi_p\rangle, \tag{4}$$

where $\mathcal{A}$ is the antisymmetrizer and φ_p is a trial scattering orbital. In the static-exchange plus polarization (SEP) approximation, the variational expansion is augmented with virtual target excitations:

$$|\chi_{mn}\rangle = \mathcal{A}|\Phi_m\rangle|\varphi_n\rangle, \tag{5}$$

where φ_n is a trial scattering orbital and Φ_m is a singly excited target state with either singlet or triplet spin coupling, though only $(N+1)$-electron configurations with total spin 1/2 (doublets) are taken into account. Modified virtual orbitals (MVO's) [22] generated in the field of cations with charge +6 were employed to represent particle and scattering orbitals.

Two levels of polarization were adopted, both constructed from virtual excitations from all the valence occupied orbitals, and allowing for singlet and triplet spin couplings. In the SEP-1 approximation, all MVO's were considered as particle orbitals in symmetry-preserving excitations, while only the lowest-lying MVO in each irreducible representation was taken as the scattering orbital. The SEP-2 approximation employs an augmented variational space, wherein the n lowest-lying MVO's were used as both particle and scattering orbitals to build symmetry-adapted CSF's. We considered a set of $n = 45$ and 30 MVO's for DMS and DMDS, respectively, such that the number of configurations in each symmetry did not exceed ≈12 000, as summarized in Table I.

TABLE I. Number of configurations employed in the SE, SEP-1, and SEP-2 approximations, for DMS (C_{2v} point group) and DMDS (C_1 point group). For DMS, we also indicate the number of configurations per irreducible representation.

		SE	SEP-1	SEP-2
DMS	Sum	159	1499	46 540
	A_1	54	389	12 300
	A_2	27	362	11 468
	B_1	32	367	11 386
	B_2	46	381	11 386
DMDS		184	2254	11 855

Unless stated otherwise, the calculations were performed at the ground-state equilibrium geometries of the target molecules, optimized at the Hartree-Fock (HF) approximation with the 6-311++G(d,p) basis set, employing the GAMESS package [23]. The nuclei and core electrons of the carbon ($1s^2$) and sulfur ($1s^2 2s^2 2p^6$) atoms were replaced by the pseudopotentials of Bachelet *et al.* [24] in the bound-state and scattering calculations. The target electronic ground state was described at the HF level, with a set of Cartesian Gaussian basis sets whose exponents are given in Table II for the sulfur and carbon atoms. For hydrogen, we employed the 3s basis set given by Poirier *et al.* (see Table 1.25.3 in Ref. [25]), augmented with one diffuse s-type orbital and one p-type orbital. The corresponding exponents (contraction coefficients) are 13.36150 (0.13084), 2.01330 (0.92154), 0.45380 (1.0), 0.12330 (1.0), and 0.03080 (1.0) for s-type orbitals and 0.75000 (1.0) for the p-type orbital. After excluding the $(x^2 + y^2 + z^2)$ combinations of Cartesian d-type functions, we obtained a total of 136 molecular orbitals for DMS and 166 for DMDS.

The calculated dipole moments of the target molecules are 1.82 D for DMS and 2.3 D for DMDS. These are overestimated with respect to the experimental values of 1.50 D [26] and 1.85 D [27], as expected for HF estimates. For DMS the long-

TABLE II. Exponents of the s-, p-, and d-type Gaussian atomic orbitals employed in the target and scattering calculations in DMS and DMDS (in units of a_0^{-2}).

Atom	s	p	d
S	7.382257	6.757373	0.476317
	2.063167	2.086910	0.151558
	0.878009	0.692726	
	0.245161	0.268602	
	0.061630	0.095936	
	0.015560	0.021486	
C	12.49628	4.911060	0.603592
	2.47029	1.339766	0.156753
	0.61403	0.405859	
	0.18403	0.117446	
	0.03998		

range dipole potential was accounted for through the Born-closure procedure described elsewhere [28]. As discussed below, the large background arising from the dipole potential could hide the signatures of shape resonances in the integral cross section (ICS) and ET spectrum. The dipole corrections were not included in the calculated cross sections of DMDS to enhance the signature of the shape resonances.

III. RESULTS AND DISCUSSION

The symmetry decomposition of the elastic integral cross section for DMS is presented in Fig. 2. The SE results display prominent structures around 7 eV (B_2 symmetry), 9 eV (A_1), and 9 eV (A_2), which are shifted down to 4.2, 5.6, and 8 eV, respectively, in the SEP-1 approximation. The more thorough description of polarization effects in the SEP-2 approximation further shifts these structures to 2.6 eV (B_2), 3.7 eV (A_1), and 5.8 eV (A_2). The electron transmission (ET) spectrum reported by Dezarnaud-Dandine *et al.* [13] suggests a single structure at 3.25 eV, which they assigned to a shape resonance with σ^*_{SC} character, in consistency with the previous ET measurements [12]. To better understand this discrepancy we present in Fig. 3 the ICS (sum over symmetry components) and the Born-corrected ICS, along with the partial cross sections (symmetry components). It is clear that the two lowest-lying resonances (B_2 and A_1) overlap and give rise to a single broader structure around 3.5 eV. As a consequence, the resolution of these two anion states in ET measurements would be difficult, since the experimental data cannot be decomposed into symmetry components. In addition, the large background arising from the dipole potential, which cannot be resolved from the resonant contribution to the ET signal, would make the resolution of the B_2 and A_1 resonances even more difficult,

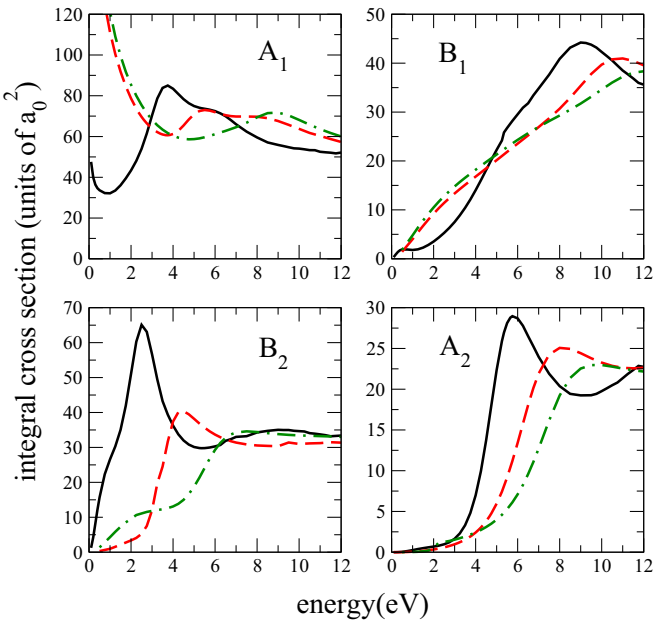

FIG. 2. (Color online) Symmetry-resolved contributions to the elastic integral cross section of DMS, obtained at SE (dotted-dashed green line), SEP-1 (red dashed line), and SEP-2 (black solid line) approximations.

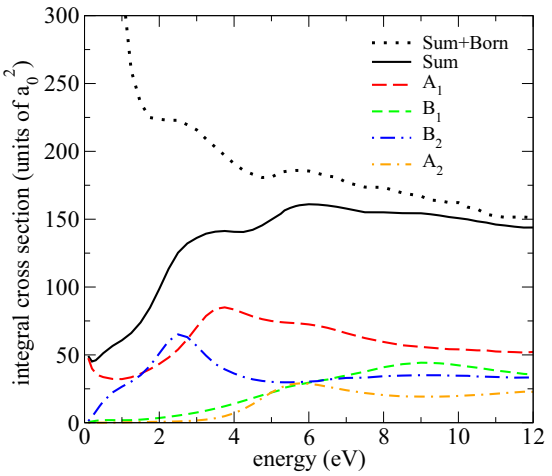

FIG. 3. (Color online) Symmetry decomposition of the elastic integral cross section for DMS, computed at the SEP-2 approximation. The integral cross section, given by the sum over symmetry components (Sum), and the Born-corrected integral cross section (Sum + Born) are also shown.

as suggested by the Born-corrected calculations. We therefore believe the experimentally assigned structure around 3.25 eV would actually arise from two superimposed resonances. While the higher-lying A_2 anion state is not evident in the ET spectrum [13], it is still discernible, although with a mild signature, in the calculated ICS and Born-corrected ICS (5.8 eV). Similar higher-lying faint structures were detected in the ET spectra of the related molecules diethyl-sulfide [12], DMDS [13], and dimethyl trisulfide [13].

Figure 4 shows the elastic ICS for DMDS, as obtained from the SE, SEP-1, and SEP-2 approximations. A shape resonance is found at 3.65 eV in the SE approximation and at 1.64 eV in the SEP-1 approximation, while a broader structure around 9 eV is present in both calculations. This fact is not surprising

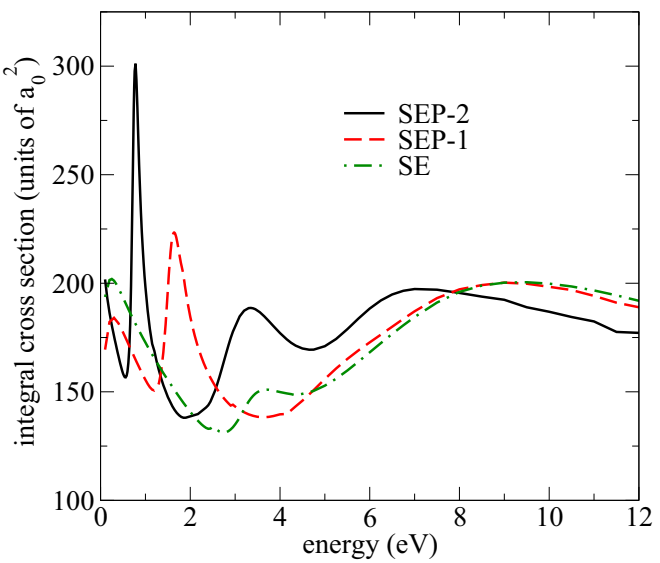

FIG. 4. (Color online) Elastic integral cross section for DMDS, obtained at SE, SEP-1, and SEP-2 approximations.

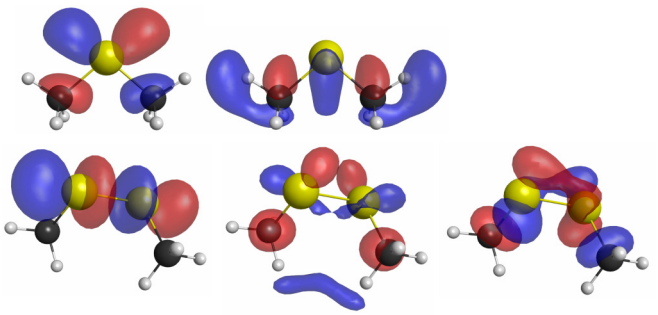

FIG. 5. (Color online) Lowest-lying virtual orbitals obtained with compact basis sets (see text). Upper panel: LUMO (left) and LUMO + 3 (right) of DMS. Lower panel: LUMO (left), LUMO + 1 (center), and LUMO + 2 (right) of DMDS.

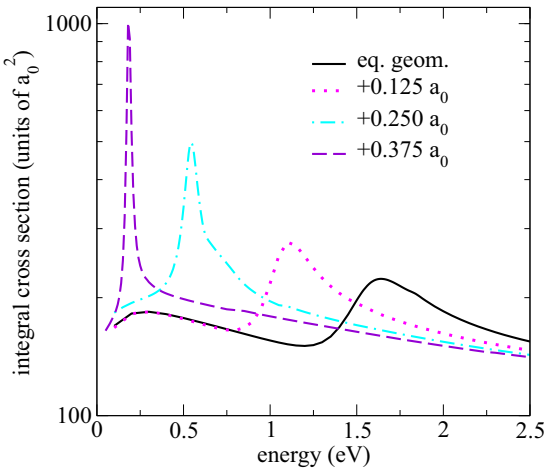

FIG. 6. (Color online) Elastic integral cross section for DMDS, obtained in the SEP-1 approximation, computed at the equilibrium geometry (black solid line), and for the stretched S–S bond lengths of 0.125 a_0 (dotted magenta line), 0.250 a_0 (dotted-dashed cyan line), and 0.375 a_0 (dashed violet line).

since only the first MVO is used as a scattering orbital in the SEP-1 procedure, thereby impacting the lowest-lying anion state more significantly. In the SEP-2 approximation, the lowest-lying resonance, having a σ^*_{SS} character (see below), is further shifted to 0.80 eV. The signature of an additional anion state around 3.3 eV also becomes evident, so we believe it was obscured by the broader and higher-lying peak (around 9 eV) in the SE and SEP-1 results. As already pointed out, the SEP-2 approximation better accounts for polarization effects and should be regarded as our most reliable result. However, the symmetry decomposition is not possible for DMDS, which belongs to the C_1 group, such that we cannot explore superimposed anion states. In spite of this limitation, there is good agreement between the present resonance energies (0.80 and 3.3 eV) and the ET data (1.04 eV and 2.72 eV) reported by Dezarnaud-Dandine *et al* [13]. Finally, the higher-lying structure shifts down to 7 eV in the SEP-2 results, and may be related in principle to the weak feature observed around 5.2 eV [13]. However, we cannot be certain, since the present elastic calculations do not account for electronic excitation or core-excited resonances.

Since the low-lying VO's obtained with compact basis sets can provide a qualitative picture of the resonance characters, we show these orbitals, as obtained from a HF/6-31G(d) calculation, in Fig. 5. For DMS we present the LUMO and the LUMO + 3, while the LUMO, LUMO + 1, and LUMO + 2 are presented for DMDS. In DMS, the LUMO (B_2 symmetry), accounting for the first shape resonance, has a clear S($3d$) character, while the LUMO + 3 (LUMO in the A_1 symmetry) has a prevailing σ^*_{SC} character on both S–C bonds and would account for the second resonance. The low-lying VO's of DMDS support the previous assignments of the resonant orbitals (see Fig. 5). The 0.80-eV feature is a shape resonance with σ^*_{SS} character, while the structure around 3.3 eV would arise from electron capture into the nearly degenerate LUMO + 1 and LUMO + 2 orbitals, both with σ^*_{SC} character.

We show in Fig. 6 the ICS's obtained for several S–S stretched bond lengths, keeping the remaining geometric parameters frozen. Since we are interested in evaluating the behavior of the σ^*_{SS} resonance, these calculations were performed at the less computationally expensive SEP-1 approximation. In consistency with the antibonding character of the σ^*_{SS} orbital, the resonance is stabilized upon stretching of the disulfide bond. In view of the ICS's profiles in Fig. 6, the SEP-1 approximation predicts that the σ^*_{SS} anion would become bound around 0.4 a_0. However, assuming that the 0.8-eV shift between the SEP-2 and SEP-1 calculations at the equilibrium geometry would also apply to the other bond lengths, the stabilization would take place around 0.2 a_0. The extension of the Franck-Condon region for the S–S stretch mode can be obtained from the characteristic length constant for the harmonic oscillator, $2\beta = 2\sqrt{\hbar/m\omega} = 0.24\,a_0$. DEA thus efficiently operate through the accommodation of $\lesssim$1 eV electrons into the σ^*_{SS} orbital followed by the disulfide bond breaking, in consistency with the strong signals for the CH_2S^- and CH_3S^- fragments [10,11]. However, as the present calculations do not allow for geometry rearrangements beyond the S–S stretching, we cannot discuss the relative abundance of the anion fragments (CH_2S^- release would be accompanied by H–S–CH_3 formation [11]). DMDS would also be expected to support a dipole-bound anion state, where the excess electron occupies a very diffuse orbital on the positive end of the molecule, which could in principle give rise to DEA mediated by vibrational Feshbach resonances. However in this case the electron would be accommodated around the hydrogen atoms and the coupling to the σ^*_{SS} valence state would be unfavorable. We thus believe the ion yield at low energies ($\lesssim$1 eV) would result from different dissociation mechanisms arising from the formation of the σ^*_{SS} anion.

IV. CONCLUSIONS

Elastic integral cross sections for collisions of low-energy electrons with dimethyl sulfide and dimethyl disulfide were calculated. The results for dimethyl sulfide allowed us to interpret the broad structure observed around 3.25 eV in the ET spectrum [10] as arising from the overlap of a $\sigma^*(3d)$ resonance around 2.6 eV and a σ^*_{SC} shape resonance around 3.7 eV. The large background arising from the dipole

interaction also hinders the distinction between these two anion states, as their signatures become less clear. We also found a higher-lying (5.8 eV) shape resonance, possibly too broad to be detected in the ET measurements. For dimethyl disulfide, we obtained σ^*_{SS} and σ^*_{SC} shape resonances, respectively, at 0.80 and 3.3 eV, in fair agreement with the ET assignments (1.04 and 2.72 eV) [13]. Scattering calculations for stretched S–S bond lengths show the expected stabilization arising from the antibonding character of the lowest-lying resonance, suggesting the dissociative electron attachment reactions are associated with the direct cleavage of the S–S bond below 1 eV.

ACKNOWLEDGMENTS

J.S.S. acknowledges fellowships from Universidade Federal do ABC (UFABC) and Coordination for the Improvement of Higher Education Personnel (CAPES). F.K. acknowledges financial support from São Paulo Research Foundation (FAPESP). M.T.N.V. acknowledges grants from FAPESP and National Council for Scientific and Technological Development (CNPq). The calculations were performed at the Laboratory for Advanced Scientific Computation at the University of São Paulo (LCCA), the Scientific Computation Center at UFABC, and Centro Nacional de Processamento de Alto Desempenho em São Paulo (CENAPAD).

[1] G. E. Schulz and R. H. Schirmer, *Principles of Protein Structure* (Springer-Verlag, New York, 1979).
[2] S. D. Dai, C. Schwendtmayer, P. Schurmann, S. Ramaswamy, and H. Eklund, Science **287**, 655 (2000).
[3] P. Limão-Vieira, S. Eden, P. A. Kendall, N. J. Mason, and S. V. Hoffmann, Chem. Phys. Lett. **366**, 343 (2002).
[4] E. A. Drage, P. Cahillane, S. V. Hoffmann, N. J. Mason, and P. Limão-Vieira, Chem. Phys. **331**, 447 (2007).
[5] F. R. Ornellas, Chem. Phys. **344**, 95 (2008).
[6] A. G. S. de Oliveira-Filho, Y. A. Aoto, and F. R. Ornellas, J. Phys. Chem. A **113**, 1397 (2009).
[7] V. Aquilanti, M. Ragni, A. C. P. Bitencourt, G. S. Maciel, and F. V. Prudente, J. Phys. Chem. A **113**, 3804 (2009).
[8] V. Favaudon, H. Tourbez, C. Houee-Levine, and J.-M. Lhoste, Biochemistry **29**, 10978 (1990).
[9] R. A. Zubarev, N. A. Kruger, E. K. Fridriksson, M. A. Lewis, D. M. Horn, B. K. Carpenter, and F. W. J. McLafferty, J. Am. Chem. Soc. **121**, 2857 (1999).
[10] A. Modelli, D. Jones, G. Distefano, and M. Tronc, Chem. Phys. Lett. **181**, 361 (1991).
[11] C. Matias, A. Mauracher, P. Scheier, P. Limão-Vieira, and S. Denifl, Chem. Phys. Lett. **605-606**, 71 (2014).
[12] C. Dezarnaud, M. Tronc, and A. Modelli, Chem. Phys. **156**, 129 (1991).
[13] C. Dezarnaud-Dandine, F. Bournel, M. Tronc, D. Jones, and A. Modelli, J. Phys. B **31**, L497 (1998).
[14] S. Carles, F. Lecomte, J. P. Schermann, C. Desfrançois, S. Xu, J. M. Nilles, K. H. Bowen, J. Bergès, and C. Houée-Levin, J. Phys. Chem. A **105**, 5622 (2001).
[15] J. A. Gámez, L. Serrano-Andrés, and M. Yáñez, Phys. Chem. Chem. Phys. **12**, 1042 (2010).
[16] J. A. Gámez, L. Serrano-Andrés, and M. Yáñez, Int. J. Quant. Chem. **111**, 3316 (2011).
[17] J. S. dos Santos, R. F. da Costa, and M. T. do N. Varella, J. Chem. Phys. **136**, 084307 (2012).
[18] K. Takatsuka and V. McKoy, Phys. Rev. A **24**, 2473 (1981); **30**, 1734 (1984).
[19] M. A. P. Lima and V. McKoy, Phys. Rev. A **38**, 501 (1988); M. A. P. Lima, L. M. Brescansin, A. J. R. da Silva, C. Winstead, and V. McKoy, *ibid.* **41**, 327 (1990).
[20] R. F. da Costa, F. J. da Paixão, and M. A. P. Lima, J. Phys. B **37**, L129 (2004).
[21] M. H. F. Bettega, L. G. Ferreira, and M. A. P. Lima, Phys. Rev. A **47**, 1111 (1993).
[22] C. W. Bauschlicher, J. Chem. Phys. **72**, 880 (1980).
[23] M. W. Schmidt, K. K. Baldridge, J. A. Boatz, S. T. Elbert, M. S. Gordon, J. H. Jensen, S. Koseki, N. Matsunaga, K. A. Nguyen, S. J. Su, T. L. Windus, M. Dupuis, and J. A. Montgomery, J. Comput. Chem. **14**, 1347 (1993).
[24] G. B. Bachelet, D. R. Hamann, and M. Schlüter, Phys. Rev. B **26**, 4199 (1982).
[25] R. Poirier, R. Kari, and I. Csizmadia, *Handbook of Gaussian Basis Sets: A Compendium for Ab-Initio Molecular Orbital Calculations*, Physical Sciences Data Vol. 24 (Elsevier, Amsterdam, 1985).
[26] L. Pierce and M. Hayashi, J. Chem. Phys. **35**, 479 (1961).
[27] R. David and E. Lide, *Handbook of Chemistry and Physics* (CRC, Boca Raton, 2003), Vol. 84.
[28] E. M. de Oliveira, R. F. da Costa, S. d'A. Sanchez, A. P. P. Natalense, M. H. F. Bettega, M. A. P. Lima, and M. T. do N. Varella, Phys. Chem. Chem. Phys. **15**, 1682 (2013).